Full life property of surface charge accumulation on HVDC spacers considering transient and steady states

Full life property of surface charge accumulation on HVDC spacers considering transient and steady states

in *IEEE Transactions on Dielectrics and Electrical Insulation*, vol. 26, no. 5, pp. 1686-1692, Oct. 2019

The final published version is available online at:https://doi.org/10.1109/TDEI.2019.008243

Full Life Property of Surface Charge Accumulation on HVDC Spacers Considering Transient and Steady States

Chuanyang Li
Department of Electrical, Electronic, and Information Engineering "Guglielmo Marconi", University of Bologna, Viale Risorgimento 2, Bologna, 40136, Italy

Baojia Deng, Zi Zhang, Wu Yan, Qiuye Li and **Zhousheng Zhang**
School of Electrical Engineering, Shanghai University of Electric Power
Changyang Road #2588, Shanghai, 200090, China

Chuanjie Lin and **Yao Zhou**
State Key Laboratory of Power Systems, Department of Electrical Engineering
Tsinghua University, Beijing 100084, China

Tao Han, Zhipeng Lei, Simone Vincenzo Suraci and **Davide Fabiani**
Department of Electrical, Electronic, and Information Engineering "Guglielmo Marconi", University of Bologna, Viale Risorgimento 2, Bologna, 40136, Italy

ABSTRACT

A theoretical model considering the dynamic change of surface charge accumulation in transient and steady states is proposed. The surface charge accumulation under transient and steady states are simulated using three model spacers with different volume conductivities. The results show that on the convex surface of a spacer, when the volume conductivity is lower than 2×10^{-18} S/m, the hetero-polarity charge accumulated on the spacer surface is dominant, while the homo-polarity charge accumulated on the surface is dominant when the conductivity is higher than 6×10^{-17} S/m. The surface charge density is non-uniformly distributed, and the time duration of the transient process of the surface charge density at different positions on the spacer surface is different, due to the distribution of electric field lines. It is hopefully that the content of this paper can provide reference for the mechanism study of gas-volume interface charge transport and the preparation of HVDC spacers.

Index Terms — **HVDC, GIL, spacer, surface charge accumulation, electric field, transient analysis**

1 INTRODUCTION

GAS insulated transmission line (GIL) serves as an optional replacement for overhead power transmission lines and has been widely used in AC electrical power transmission systems. However, the surface charge accumulation on spacers are believed to be a significant threat to the stable operation of DC GIL [1]. The operating environment of the spacer surface inside DC GIL is a typical gas-volume interface. Due to the distribution of DC electric field lines, charges in the volume and in SF_6 are pushed and accumulate in the interface where a vertical electric field component touches the surface [2]. The problem of surface charge accumulation is considered as one of the core issues limiting the development of gas insulated transmission technology under DC [3].

The charge generation on the surface of spacers inside a GIL is generally considered to have the following three sources: the conduction along the surface of the spacer (surface conduction), the conduction through the bulk of the spacer (volume conduction) and the gas volume conduction (gas conduction). The competitive relationship between the three parts is depended by the electric field distribution [4], the geometry of the insulation system [5,6], ion pair generation rate[5,6] and other charge carriers generated under high field conditions [6-9]. In previous studies, during the calculating of the electric field distribution and surface charge distribution of a spacer, the generation and transport of ions in SF_6 are mostly based on the fluid dynamic equation of the gas discharge theory. In addition, most of current researches focus on the steady state characteristics of surface charge behavior [10-13]. However, very few studies discuss the charge behavior in combination with transient and steady states during charge

accumulation process. In the existing transient analysis, the description of full-life process of charge accumulation is not fully integrated with electric field distribution with capacitance during initial transient process and electric field with resistance variation in the steady state, after the voltage is applied for a long time [14, 15].

This paper studies the full-life behavior of surface charge accumulation considering the process of transient and steady states. The transient distribution and steady state distribution of the charge accumulation on the spacer surface using three model spacers with different volume conductivities are discussed. It is hopefully that this paper can provide a useful reference for the mechanism study of gas-volume interface charging and the manufacturing of HVDC spacers.

2 THEORETICAL MODEL

Figure 1 shows the two-dimensional axisymmetric simplified model of a GIL spacer. The time derivative of the surface charge density $\sigma(z,t)$ at any point $P(z)$ of the spacer surface can be obtained by the modified Maxwell continuity equation for a thin layer covering the spacer surface [16]

$$-\frac{\partial\sigma(z,t)}{\partial t}=J_{G(z,t)}-J_{I(z,t)}-J_{S(z,t)} \tag{1}$$

where σ(z,t) is the surface charge density, C/m^2; $J_{G(z,t)}$, $J_{I(z,t)}$ and $J_{S(z,t)}$ are the electrical conductance density of the spacer surface due to the gas conductance, the volume electrical conductivity flow density and the surface current density in this thin surface layer, A/m^2.

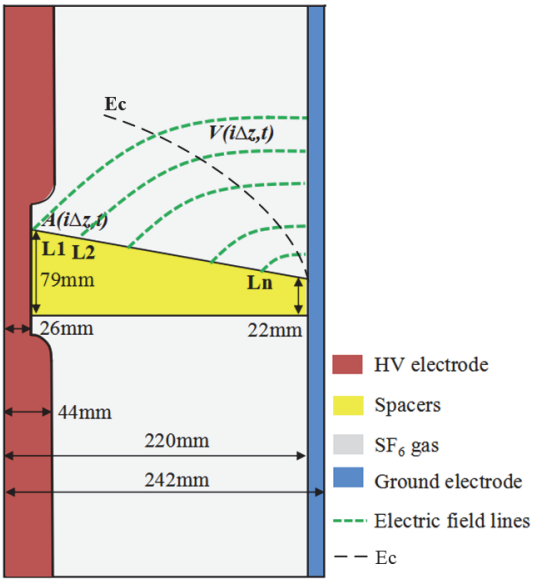

Figure 1. Two-dimensional axisymmetric simplified model of GIL spacer.

The surface of the spacer studied in this paper is not a modified one, and as a consequence, the $J_{S(z,t)}$ term in Equation (1) can be ignored according to [4]. The volume conductivity of the spacer is calculated using Ohm's law

$$J_{I(z,t)}=E_{I(z,t)}\delta \tag{2}$$

where $E_{I(z,t)}$ represents the normal electric field intensity of the volume side, V/m; δ represents the conductivity of the volume state, S/m.

$J_{G(z,t)}$ is determined by physical parameters such as the gas ion generation rate, the mobility, and the composite coefficient. E_c is defined as the critical field strength threshold of the ion recombination value. According to the structural characteristics of the GIL system, in the GIL system, ion recombination occurs in a region where the electric field strength is smaller than E_c, and only ions in the region where the electric field strength is greater than E_c can all move to the surface of the spacer, and surface neutralization occurs to form a surface charge. The area that is stronger than E_c is the area studied in this paper and is defined as the effective area. Therefore, the dynamic change of the ion recombination rate is not considered in the mathematical model of the gas ion current density.

Since $J_{G(z,t)}$ is non-uniformly distributed on the spacer surface, the surface is divided into n partial surfaces $A_{(i\cdot\Delta z,t)}$ equally. The upper and lower boundaries of the local surface are defined as the power lines that cross the gas-spacer interface when $z=i\cdot\Delta z$ and $z=(i+1)\cdot\Delta z$. Moreover, the two power lines together with the E_c boundary line and the partial surface constitute a local gas volume $V_{(i\cdot\Delta z,t)}$. After the above definition of local surface and local volume, the two-dimensional diagram in Figure 1 is equivalent to divide the spacer surface from the high voltage side to the low voltage side into n equal segments, marked as L1, L2·· Ln. The length of each segment is Δz. Since the electric field generated by the surface charge is superimposed on the external electric field during the charging process, the electric field distribution changes dynamically with time. Therefore, the local volume $V_{(i\cdot\Delta z,t)}$ is a function of time. This paper considers the movement of ions along the electric power line in the volume. When the electric field strength is less than the critical field strength E_c, the ions have a recombination process. When the electric field strength is higher or equal to E_c, the gas ions generated by natural ionizing radiation can reach the surface of the spacer and ignore the recombination process. This paper only considers the area where the electric field strength is greater than E_c. The mathematical model of the gas conductivity density of the local surface is thereby established as:

$$J_{G(i\cdot\Delta z,t)}=\frac{Ne}{A_{(i\cdot\Delta z,t)}}V_{(i\cdot\Delta z,t)} \tag{3}$$

where N is the ion pair generation rate, IP/(cm^3 · s); e is the unit charge amount, C; $V_{(i\cdot\Delta z,t)}$ is the space effective volume with electric field strength greater than E_C , m^3; $A_{(i\cdot\Delta z,t)}$ is the area corresponding to the effective neutralization volume on the spacer, m^2.

During simulation, the spacer is divided into 20 small cells along the surface. In the simulation, the voltage value is +500 kV, and the ion pair generation rate is N=29, IP/(cm^3·s). The electrical conductivity of the spacer is separated into high, medium and low sections with values in range of 10^{-19}-10^{-17} S/m [15]. The solid conductivity selected in this paper is

around the range of pure epoxy resin (undoped): 2×10^{-18} S/m, 9×10^{-18} S/m and 6×10^{-17} S/m, respectively. The values of the basic parameters in the simulation are shown in Table 1.

Table 1. Values of the basic parameters in the simulation of GIL.

Physical quantity	Name	Numerical value	Unit
e	Unit charge	1.6×10^{-19}	C
ε(epoxy)	Dielectric constant	4.95	--
ε(SF_6)	Dielectric constant	1.002	--

3 ITERATIVE ALGORITHM

The simulation tools used in this paper are COMSOL and MATLAB. The finite element method (FEM) is used to simulate and calculate the electromagnetic field. The partial differential equation (PDE) calculation function of COMSOL and the cyclic call function of MATLAB are both applied.

Three subroutines are developed. The first subroutine is to draw electric power lines starting at a distance of Δz originated from $z=i\cdot\Delta z$ on the spacer surface, and to calculate the normal electric field intensity $E_{I(z,t)}$ in the volume side. After considering the electric field line distribution and rotational symmetry, the second subroutine calculates the local gas volume $V_{(i\cdot\Delta z,t)}$ and the gas side current density according to $J_{G(i\cdot\Delta z,t)}$. The third subroutine is used to extract the normal electric field strength $E_{I(z,t)}$ inside the spacer surface and calculate the volume current density $J_{I(z,t)}$ according to the volume current density equation.

For the discretization of the dynamic calculation model, firstly, time integration is calculated based on Equation (1):

$$\delta(z,t)=\int_0^t\left(J_{I(z,t)}-J_{G(z,t)}\right)dt \tag{4}$$

After discretization of Equation (4), the following equation can be obtained:

$$\delta\left(z,(j+1)\cdot\Delta t\right)=\sum_{j=0}^{\infty}\left(J_{I(z,j\cdot\Delta t)}-J_{G(z,j\cdot\Delta t)}\right)\cdot\Delta t \tag{5}$$

where $j\geq0$, $\delta(z,0)=0$.

The iterative calculation method of Equation (5) is used to calculate the transient accumulation process of surface charges. Each iteration step includes the calculation of electrostatic field J_G and the calculation of current density J_I. The current density difference between the volume side and the gas side in the geometric series is calculated by three subroutines developed by the j_{th} iteration and the developed subroutine, taking into account the surface charge density that is accumulated during the $(j-1)_{th}$ iteration. This means that in addition to the boundary voltage values of the high voltage terminal voltage V_0 and the low-voltage terminal voltage 0, the non-uniform distribution and cumulative increased surface charge density $\delta(z,(j),\Delta t)$ are defined as a new boundary conditions after each iterations. Therefore, the electric field generated by the accumulated surface charge is superimposed on the external field.

The ideal conditions for the end of the iteration are as follows:

$$J_{I(z,t)}-J_{G(z,t)}=0 \tag{6}$$

A very small value (10^{-13}) was chosen as the current density difference to ensure the accuracy of the iteration calculation.

4 SIMULATION RESULTS

4.1 TRANSIENT STATE ANALYSIS

The transient property of spacers refers to the feature of surface charge variation, including the charge quantity and amplitude changing with time, T_w (the time when surface charge accumulation reaches stable), and the distribution changes of the electric field lines in SF_6 with time.

The change of charge density on the spacer surface with time during the transient process is shown in Figure 2. When the conductivity of the spacer is 2×10^{-18} S/m as shown in

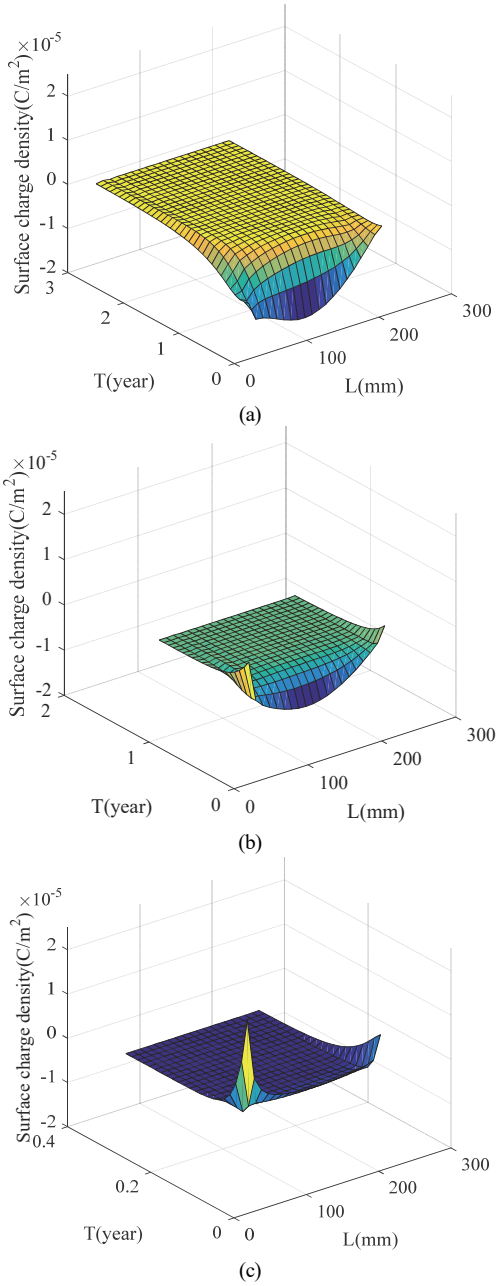

Figure 2. The change of charge density increment on the spacer surface with time during the transient process; (a) volume conductivity of 2×10^{-18} S/m, (b) volume conductivity of 9×10^{-18} S/m, and (c) volume conductivity of 6×10^{-17} S/m.

Figure 2a, only negative charges accumulate on the spacer surface. The stable time for charge accumulation at different locations on the spacer surface is different, due to the competition between normal field strength distribution on the volume side and on the gas side. We define a time value to which the accumulated charge density reach 90% of the stable value of the charge density. Then the steady state time of sample with a conductivity of 2×10^{-18} S/m is 2.8 years. When the conductivity is increased to 9×10^{-18} S/m as shown in Figure 2b, charges with positive and negative polarity both exist on the surface. A positive charge is easily accumulated at a position close to the electrode, and a negative charge is easily accumulated at a position away from the electrode. The steady-state time of this sample is decreased to 1.1 years. The same polarity charge dominates when the volume conductivity increase to 6×10^{-17} S/m shown in Figure 2c. The accumulation of charge at the electrodes is more pronounced.

Figure 3 shows the variation of the electric field line distribution using different experimental samples. For the sample with a volume conductivity of 2×10^{-18} S/m, the electric field line distribution inside the spacer gradually changes from a dense distribution to a sparse distribution, during the process when charge accumulation process was transited from the transient state to the steady state. However, the distribution property of electric field lines on the gas side is different, which shows a change trend from a sparse distribution to a dense distribution with the increasing of time. The model spacer with a bulk conductivity of 9×10^{-18} S/m shows less variation in electric power line distribution during transient process compared with that of the model spacer with a bulk conductivity of 2×10^{-18} S/m. The electric field line distribution in the volume becomes slightly sparse with the increase of time, while it remains almost unchanged in the gas side. For samples with a bulk conductivity of 6×10^{-17} S/m, the initial electric field line distribution in the volume is denser than that compared with the gas side. As the time increases, the electric power line distribution in the volume gradually becomes denser, while the electric field line distribution remains almost unchanged in the gas side.

The surface charge density is determined directly due to the distribution of normal composite of the electric field lines. Figure 4 shows the normal electric field component along the surface at different times for different samples. It can be found that the normal electric field component is relatively high near both electrodes, especially at the high voltage electrode, which

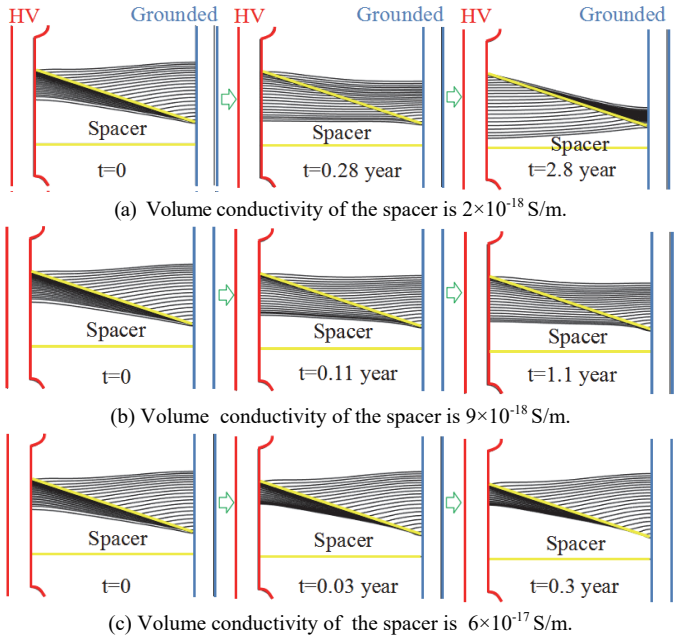

Figure 3. Variation of electric field line distribution on insulator surface during transient to steady state.

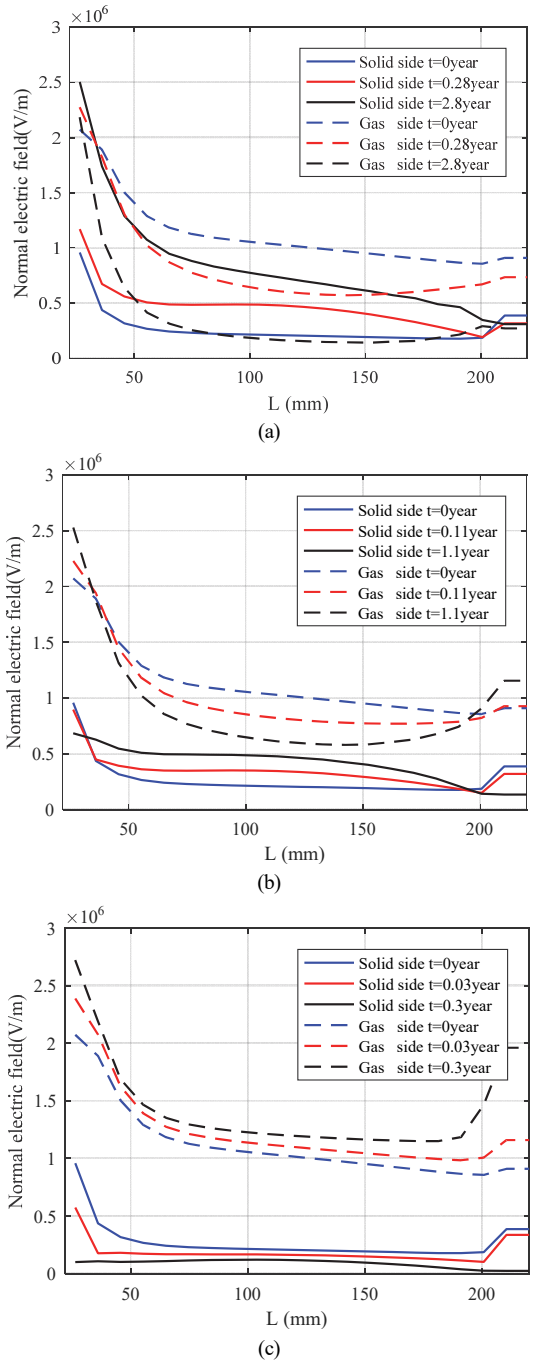

Figure 4. Normal composite of electric field lines for different samples; (a) volume conductivity of the spacer is 2×10^{-18} S/m, (b) volume conductivity of the spacer is 9×10^{-18} S/m, (c) volume conductivity of the spacer is 6×10^{-17} S/m.

is a common rule of the three model spacers. In addition, the amplitude of the normal component of the electric field line in the gas side is larger than that compared with the amplitude of the normal component in the volume side. However, this rule does not include the sample with a conductivity of 2×10^{-18} S/m, especially for electric field lines at the volume during the steady state. For samples with conductivity values of 2×10^{-18} S/m and 6×10^{-18} S/m, the normal electric field component of the gas side decreases with time, and the normal electric field component of the volume side increases with time. While an opposite trend is found for the model spacer with a conductivity of 6×10^{-17} S/m. Considering the distribution characteristics, the change of the normal electric field component with time and with higher conductivity tends to be inconspicuous. This feature is more obvious in the sample with a conductivity value of 6×10^{-17} S/m.

4.2 STEADY STATE ANALYSIS

The steady state characteristic of spacers refers to the state when a stability is reached for charge accumulation. Due to the physical structure and material properties of the spacer-electrode system, when the surface charge accumulation reaches steady state, charges with different polarities and amplitudes are accumulated at different positions on the spacer surface. The steady-state charge distribution along the surface of the spacer with 3 typical conductivities can be found in Figure 5. When the spacer conductivity is 2×10^{-18} S/m, the surface of the spacer mainly accumulates negative charges. The closer to the center conductor, the greater the negative surface charge density is found, and the maximum negative charge density is -8.61×10^{-5} C/ m^2. When the volume conductivity is 9×10^{-18} S/m, there are positive and negative charges on the surface of the spacer. It is easier for the surface to accumulate positive charges near the surface near the high voltage conductor, and negative charges near the ground electrode. When the volume conductivity is 6×10^{-17} S/m, the surface charge distribution of the spacer is a uniformly distributed with positive charges with a lower amplitude of charge density.

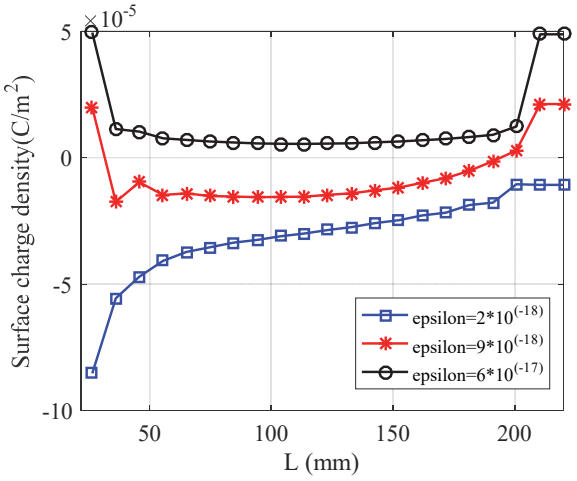

Figure 5. Steady-state charge distribution of spacer surface; (a) volume conductivity 2×10^{-18} S/m, (b) volume conductivity 9×10^{-18}S/m, (c) volume conductivity 6×10^{-17}S/m.

5 DISCUSSION

The magnitude and direction of current density on the spacer surface determines the polarity and magnitude of surface charge. It is defined in this paper that the directions of the current density in volume-state and gas-side are consistent with the direction form the spacer side pointing to the gas side. Therefore, the polarity of surface charge depends on the direction of the volume side and gas side current density vectors. If the gas side normal current density modulus is larger than the volume side normal current density modulus, the current density vector direction would be negative, and the surface mainly accumulates a negative charge. At this time, the gas side dominates the surface charge accumulation of the spacer. If the volume side normal current density modulus is greater than the gas side normal current density modulus, then the direction of the current density vector sum is positive. The surface mainly accumulates a positive charge, and the positive charge on the volume side would be a dominant contribution in the surface charge accumulation process of the spacer. From the simulation calculation results (Figure 2), when the volume conductivity is 2×10^{-18} S/m, the charging from the gas side serves as the dominant factor of charge accumulation. When the volume conductivity is 9×10^{-18} S/m, the sum of the gas side and the volume side vector is minimized, and the contribution of both on the surface charge accumulation is nearly equivalent. When the volume conductivity is as large as 6×10^{-17} S/m, the charging from the volume side would be the dominant factor for charge accumulation.

After the charge accumulation reaches a steady state, if the applied DC voltage and ion generation rate are constant, in case the volume side charge source is dominant, to continue to increase the volume conductivity will not change the positive charge accumulated. This is equivalent to increasing the temperature of the spacer environment after the surface charge accumulation reaches a steady state. The temperature gradient promotes the cohesion of the homo-polarity charges on the surface area, expanding the area of the “analogous ineffective region” [20]. It could be explained either in case, i.e. to increase the gas mobility does not change the charge polarity during steady state when the gas side dominates surface charge polarity.

Figure 6 shows the electric field strength along the spacer surface with different electrical conductivities (without considering the uneven distribution of trap density of volume materials, and the surface treatment of materials) [21-23]. It can be seen that the surface electric field strength gradually increases with the decrease of the distance from the high voltage electrode, and this phenomenon is more obvious in the sample with low conductivity. As the conductivity of the insulator increases, the electric field strength gradually decreases, and the electric field gradually becomes uniform along the surface distribution. The surface field strength is substantially stable when the conductivity is greater than 6×10^{-17} S/m. This indicates that when the conductivity is greater than a certain degree, the effect of the increase in conductivity on the steady-state electric field strength will be very small.

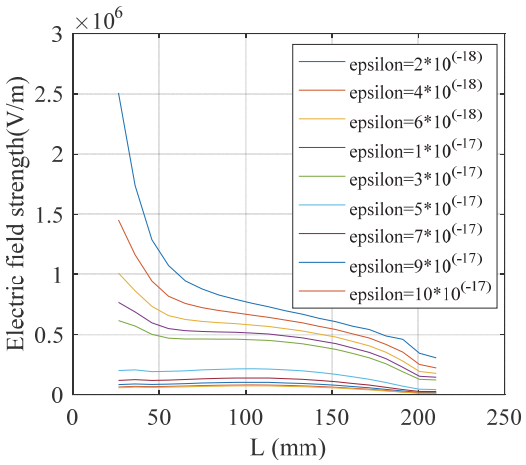

Figure 6. Electric field distribution along the spacer surface with different conductivity after steady state.

However, it is worth noting that the temperature gradient in the spacer is existed, and the temperature is an important factor affecting the conductivity of the spacer [17, 18]. The discussion of surface charge accumulation referring to volume conductivity should not be done without considering temperature gradients. The most straightforward way to reduce the effects of temperature gradients is to decrease the temperature dependence of the conductivity of the material. Our previous research proposed a method for suppressing temperature gradient expansion by doping a heat-resistant material [18]. In addition, a charge adaptive spacer can also be used in this case [3]. The spacer with continuous change of conductivity can also be obtained by 3D printing and FGM technology, thereby reducing the influence of the surface charge change of the spacer on the electric field distortion under the temperature gradient [17]. However, all of the above are performance studies using small samples in the laboratory. Before industrialization, large-scale insulators are required for thorough verification, especially aging tests. Before that, there is still a lot of basic work to be done.

6 CONCLUSION

This paper develops a theoretical model considering the dynamic change of surface charge accumulation in transient and steady states. The conclusions are as follows:

(1) The polarity and density of the accumulated surface charge are related to the competition of the charge transport in volume side and in gas side. When the volume conductivity is 2×10^{-18} S/m, the gas side is dominant. When the conductivity of volume is 9×10^{-18} S/m, both gas and volume play a key role into determining of surface charge property. When the conductivity of volume is 6×10^{-17} S/m, the volume side is the dominant factor of surface charge accumulation.

(2) The charge density is non-uniform distribution on the spacer surface, and the transient time of charge density is different at different positions on the spacer surface. The hetero polarity charge is more likely to accumulate on the spacer surface near the center conductor. The homo polarity charge tends to accumulate on the spacer surface near the ground enclosure.

(3) The surface electric field strength decreases and gradually stabilizes with the increase of volume conductivity, after the steady state is reached. When the conductivity is higher than 6×10^{-17} S/m, the electric field distribution becomes uniform. However, the key consideration in this case would be the disadvantage of leakage current.

ACKNOWLEDGMENT

This work was supported in part by the National Natural Science Foundation of China (Grant No. 51677113,51737005).

REFERENCES

[1] J. Xue, H. Wang, J. Chen, K. Li, Y. Liu, B. Song, and G. Zhang, "Effects of surface roughness on surface charge accumulation characteristics and surface flashover performance of alumina-filled epoxy resin spacers," J. Appl. Phys., vol. 124, 083302 , 2018.

[2] C. Y. Li, J. Hu, C. J. Lin, B. Y. Zhang, G.X. Zhang and J. L. He, "Surface Charge Migration and dc Surface Flashover of Surface-modified Epoxy-based Insulators," J. Phys. D: Appl. Phys., vol. 49, p. 445304, 2017.

[3] C.Y. Li, C.J. Lin, J. Hu, W.D. Liu, Q. Li, B. Zhang, S. He, Y. Yang, F. Liu, and J.L. He, "Novel HVDC Spacers by Adaptively Controlling Surface Charges – Part I: Charge Transport and Control Strategy," IEEE Trans. Dielectr. Electr. Insul., vol. 25, no. 4, pp. 1238–1247, 2018.

[4] B. Lutz, and J. Kindersberger, "Surface charge accumulation on cylindrical polymeric model spacers in air: Simulation and Measurement," IEEE Trans. Dielectr. Electr. Insul., vol. 18, no. 6, pp. 2040–2048, 2011.

[5] J. Kindersberger, and C. Lederle, "Surface Charge Decay on Spacers in Air and Sulfurhexafluorid–Part I: Simulation," IEEE Trans. Dielectr. Electr. Insul., vol. 15, no. 4, pp. 941–948, 2008.

[6] J. Kindersberger and C. Lederle, "Surface charge decay on spacers in air and sulfurhexafluorid–Part II: Measurement," IEEE Trans. Dielectr. Electr. Insul., vol. 15, no. 4, pp. 949–957, 2008.

[7] S. Okabe, "Phenomena and mechanism of electric charges on spacers in gas insulated switchgears," IEEE Trans. Dielectr. Electr. Insul., vol. 14, no. 1, pp. 46–52, 2007.

[8] C.Y. Li, C.J. Lin, Y. Yang, B. Zhang, W.D. Liu, Q. Li, J. Hu, S. He, X.L. Liu, and J.L. He, "Novel HVDC Spacers by Adaptively Controlling Surface Charges–Part II: Experiment," IEEE Trans. Dielectr. Electr. Insul., vol. 25, no. 4, pp. 1248–1258, 2018.

[9] C. Y. Li, C.J.Lin, G. Chen, Y.P.Tu, Y. Zhou, Q. Li,B. Zhang, and J.L.He, "Field-dependent charging phenomenon of HVDC spacers based on dominant charge behaviors," Appl. Phys. Lett., vol.114, no.20, p. 202904, 2019.

[10] A. Mohamad, G. Chen, Y. Zhang, Z.L.An, "Moisture effect on surface fluorinated epoxy resin for high-voltage DC applications," IEEE Trans. Dielectr. Electr. Insul., vol. 23, no. 2, pp. 1148–1155, 2016.

[11] M. Schueller, U. Straumann, and C. M. Franck, "Role of Ion Sources for Spacer Charging in SF_6 Gas Insulated HVDC Systems," IEEE Trans. Dielectr. Electr. Insul., vol. 21, no. 1, pp. 352–359, 2014.

[12] M. Schueller, R. Gremaud, C. B. Doiron , and C. M. Franck, "Micro discharges in HVDC gas insulated systems," IEEE Trans. Dielectr. Electr. Insul., vol. 22, no. 5, pp. 2879–2888, 2015.

[13] J.W. Zhang, D.K. Cao, Y.C. Cui, F.Wang, C.Putson, and C.Song, "Influence of potential induced degradation phenomena on electrical insulating backsheet in photovoltaic modules," Journal of Cleaner Production, vol.208, pp.333-339, 2019.

[14] A. Winter, and J. Kindersberger, "Transient field distribution in gas-volume insulation systems under DC voltages," IEEE Trans. Dielectr. Electr. Insul., vol. 21, no. 1, pp. 116–128, 2014.

[15] M. Tschentscher, and C. M. Franck, "Conduction processes in gas-insulated HVDC equipment: from saturated ion currents to micro-discharges," IEEE Trans. Dielectr. Electr. Insul., vol. 25, no. 4, pp. 1167–1176, 2018.

[16] E. Volpov, "Electric Field Modeling and Field Formation Mechanism in HVDC SF6 Gas Insulated Systems," IEEE Trans. Dielectr. Electr. Insul., vol. 10, no. 2, pp. 204–215, 2003.

[17] S. He, C.J. Lin, J. Hu, C.Y. Li, and J.L. He, "Tailoring charge transport in epoxy based composite under temperature gradient using $K_2Ti_6O_{13}$

and asbestine whiskers," J. Phys. D: Appl. Phys., vol. 51, no. 21, 215306, 2018.
[18] G.M.Ma, H.Y.Zhou, S.P.Liu, Y.Wang, S.J.Zhao, S.J.Liu, C.R.Li, and Y.P.Tu, "Measurement and simulation of charge accumulation on a disc spacer with electro-thermal stress in SF6 gas," IEEE Trans. Dielectr. Electr. Insul., vol. 25, no. 4, pp. 1221–1229, 2018.
[19] W.D.Li, X.R.Li, B.H.Guo, C.Wang, Z.Liu, and G.J.Zhang, "Topology optimization of truncated cone insulator with graded permittivity using variable density method," IEEE Trans. Dielectr. Electr. Insul., vol. 26, no. 1, pp. 1–9, 2019.
[20] C. Y. Li, J. Hu, C. J. Lin, and J. L. He, "The neglected culprit of dc surface flashover-electron migration under temperature gradients," Sci. Rep., vol.7, pp.1–11, 2017.
[21] Y. Zhou, S.M. Peng, J. Hu, and J.L. He, "Polymeric insulation materials for HVDC cables: development, challenges and future perspective," IEEE Trans. Dielectr. Electr. Insul., vol. 24, no. 3, pp. 1308–1318, 2017.
[22] J. Li, H. C. Liang, B. X. Du, and Z. H. Wang, "Surface Functional Graded Spacer for Compact HVDC Gaseous Insulated System," IEEE Trans. Dielectr. Electr. Insul., vol. 26, no. 2, pp. 664–667, 2019.
[23] C. Zhang, H. Lin, S. Zhang, Q. Xie, C. Ren, and T. Shao, "Plasma surface treatment to improve surface charge accumulation and dissipation of epoxy resin exposed to DC and nanosecond-pulse voltages," J. Phys. D: Appl. Phys., vol.50, no.40, 405203, 2017.

Chuanyang Li was born in Shandong, China, on February 6, 1987. He received his double B.S. degrees of Electrical Engineering and English in Taiyuan University of Technology. After that, he spent 3 years to obtain his M.S. degree from the Department of Electrical Engineering, Taiyuan University of Technology, from 2011 to 2014. He received his Ph.D degree in the Department of Electrical Engineering, Tsinghua University in 2018. Currently, he works as a Postdoctoral Fellow at the Department of Electrical, Electronic and Information Engineering "Guglielmo Marconi" of the University of Bologna (Alma Mater Studiorum - Università Di Bologna), Italy. His research interests include surface charge behavior, material modification for dielectrics in GIS/GIL, online monitoring of nuclear power cable insulation, and PD pattern recognition of HV motors and generators. He used to serve as the Guest Editor of the IEEE Trans. Dielectr. Electr. Insul. Special Issue on Advanced Dielectrics for Gas-Insulated Transmission Lines in 2018. He may be reached by: lichuanyangsuper@163.com.

Baojia Deng was born in Chongqing city, China, in 1992. She received the B.S. degree in electrical engineering from Shanghai University of Electric Power in 2016. Currently she is studying for the M.S. degree at Shanghai University of Electric Power, Shanghai, China. Her research interests cover insulation of volume dielectric and charge accumulation and dissipation associated with high voltage spacer under dc stress.

Zhousheng Zhang was born in Enshi city, China, in 1969. He received the B.S. degree in physics from Huazhong Normal University in 1992. He received the M.S. degree in electrical engineering from Huazhong University of Science and Technology in 1999. He received the Ph.D. degree in electrical engineering from Shanghai Jiaotong University in 2010. Currently, he is a Professor with the Shanghai University of Electric Power. His current research interests include gas discharges, electrical insulation and materials, and condition monitoring of power apparatus. He can be reached by: shengzz@shiep.edu.cn.

Chuangjie Lin was born in Sichuang, China, on July 15, 1993. He received the B.S. degree from Tsinghua University, China, in 2016. Currently, he is a Ph. D. student in the Department of Electrical Engineering, Tsinghua University. His research interests include surface charge behavior and multiphysics simulations for HVDC spacers.

Yao Zhou (S'16) was born in Shaanxi Province, China, in 1992. He received the B.Sc. degree in Electrical Engineering and the second B.Sc. degree in Economics from Tsinghua University, Beijing, China, in 2014. Currently, he is a Ph.D. candidate in the Department of Electrical Engineering, Tsinghua University. His research interests include electrical insulation materials, energy storage material and high voltage engineering.

Zhipeng Lei was born in Taiyuan, China in 1983. He received the B.Sc. degree from the East China Jiaotong University, China in 2005, and the M.Sc. degree, Ph.D. degree from the Taiyuan University of Technology, China in 2010 and 2015, respectively. He joined the College of Electrical and Power Engineering in the Taiyuan University of Technology as a lecturer since 2015. His main research interest is the condition assessment of high voltage cable failure and associated partial discharges characteristics, intelligence techniques in coal mine.

Tao Han (M'16) was born in Shandong, China. He received the M.E. and Ph.D. degrees in electrical engineering from Tianjin University, China, in 2012 and 2015, respectively. Since 2015, he has been a lecturer at School of Electrical Engineering and Automation in Tianjin University, China. His main research interests are degradation of cable insulation and partial discharge detection.

Simone Vincenzo Suraci was born in Reggio Calabria, Italy, in 1993. He received his B. Sc. Degree in Civil and Environmental Engineering from the University of Reggio Calabria in 2015 and his M.Sc. degree in Energy and Nuclear Engineering from the University of Bologna in 2017. He is now at the second year of his PhD in Electrical Engineering at the University of Bologna. His research interests include the study of polymeric dielectrics for nuclear applications and their degradation with aging, nondestructive diagnosis techniques for insulation materials and nano-structured composites. He has been member of both IEEE and DEIS since 2017.

Davide Fabiani (M'98) was born in Forli, Italy, in 1972. He received the M.Sc. (honors) and Ph.D. degrees in electrical engineering from the University of Bologna in 1997 and 2002, respectively. He is an associate professor at the Department of Electrical Electronics and Information Engineering of the University of Bologna since 2014. His research interests deal with the effects of voltage distortion on accelerating insulation degradation, characterization of insulating, magnetic, superconducting, nanocomposites and electret materials, aging investigation and diagnosis of power system insulation and, particularly, motor windings subjected to fast repetitive pulses. He is author or co-authors of about 180 papers. He is a senior member of IEEE, Power Engineering Society (PES), Dielectrics and Electrical Insulation Society (DEIS) and AEI from 1998. He is a Senior Associate Editor of the IEEE Transactions on Dielectrics and Electrical Insulation.